

RESEARCH ARTICLE

OPEN ACCESS

## A mini-review on proton conduction of BaZrO<sub>3</sub>-based perovskite electrolytes

<sup>1</sup>ganeswar Sahu, <sup>2</sup>satyaranjan Sethi,

Gandhi Institute of Excellent Technocrats, Bhubaneswar  
Zenith Institute of Sciences Technology, Khurda, Odisha, India

### ABSTRACT

Proton conducting ceramics show promise in fuel cells, electrolyzers, permeation membranes, sensor applications, and membrane reactors. Among several types of materials that exhibit proton conduction, perovskite oxides show high proton conductivity at intermediate temperatures, presenting potential benefits for long-term use and lower costs for energy applications. Doped barium zirconate, BaZrO<sub>3</sub>, is a material that has shown high proton conductivity with encouraging chemical stability. Therefore, it is considered a promising material especially for proton-conducting solid oxide electrochemical cells. Although the proton conduction of doped BaZrO<sub>3</sub> has been extensively characterized, the specific phenomena behind its proton conduction are not fully understood. Only recently have specialized techniques and computational tools begun to elucidate the phenomena that determine the conduction properties of the material. In this mini-review, an evaluation of the factors affecting the proton conductivity of doped BaZrO<sub>3</sub> perovskites and the phenomena governing variations in proton concentration and mobility are presented.

Special attention is given to proton interactions with dopants and their resulting effect on hydration and transport properties. Technical strategies are provided to give some guidance on the development of protonic ceramics in energy conversion applications.

**Keywords:** proton conductor, perovskite ceramics, hydration thermodynamics, proton concentration, proton trapping, solid oxide cells

### INTRODUCTION

The interest in proton-conducting ceramics has continuously grown since the 1980s when proton conduction was first observed in doped SrCeO<sub>3</sub> oxides at high temperatures (>600°C) in a humidified atmosphere [1,2]. Later on, some new materials such as nobates [3], tantalates [3], perovskites, and disordered perovskites [4,5], were shown to exhibit proton conductivity. Each material family demonstrated its own special characteristics, requiring a deeper understanding of each to optimize proton conduction for a given application. The applications of proton-conducting ceramics are diverse: sensors, hydrogen separation membranes, fuel cells, steam electrolyzers, and membrane reactors [6–11]. In particular, there has been significant recent interest in their use in solid oxide electrolysis cells (SOECs) for hydrogen production. The SOECs based on proton-conducting electrolytes, the proton-conducting SOECs (p-SOECs), can deliver pure hydrogen with some critical advantages over conventional oxide-ion conducting SOECs: reduced operating temperature, absence of nickel oxidation, and dry hydrogen production without the need for further separation [12–

19]. Additionally, with the high proton conductivity of these conductors and the optimization of composition and fabrication, the electrolysis current density has been increasingly improved. Still, the development of electrolytes remains challenging due to a restrained total conductivity, chemical stability, and the electronic conduction under gas conditions which can reduce current efficiency

[1,16,17,20,21]. Furthermore, consideration on potential electronic leakage during electrolysis operation, as found in recent works [16, 17, 21, 22], has become an additional concern that can be addressed by revealing the mechanism of the electronic conduction and developing new protonic ceramics. To better address these technical concerns, it is important to understand the underlying mechanism of

proton conduction to promote innovations in electrolyte composition for practical operation at low temperatures.

Proton conduction is a temperature-activated process and is observed in water-containing atmospheres as a function of gas at  $50^{\circ}\text{C}$ . Equation (1) shows the relationship of proton conductivity ( $\sigma_{\text{OH}^-}$ , Sm<sup>-1</sup>)

with temperature following an Arrhenius type dependence,

$$\sigma = \sigma^* \exp \left( -\frac{E_a}{kT} \right) \quad (1)$$

where  $\sigma^*$  is the pre-exponential factor describing proton conductivity ( $\text{Sm}^{-1}$ ),  $E_a$  is the activation energy for proton conduction (eV),  $k$  is the Boltzmann constant, and  $T$  is the temperature (K).

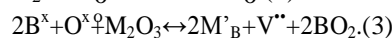
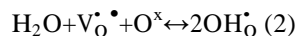
Among several proton-conducting perovskites developed in the past decades, doped  $\text{BaCeO}_3$  and  $\text{BaZrO}_3$  have shown the most promising application potential due to their high proton conductivity, chemical stability, and fabrication feasibility [5, 16, 23–27]. Perovskite systems containing  $\text{Ce}(\text{BaCeO}_3)$  and  $\text{BaCe}_{1-x}\text{Zr}_x\text{O}_3$  exhibit high conductivity [23, 24, 28]. However, their low chemical stability in steam and  $\text{CO}_2$  gases is a subject of concern [29–33]. In contrast, several studies have shown that  $\text{BaZrO}_3$  is stable in steam and  $\text{CO}_2$  and does not form  $\text{BaCO}_3$  and  $\text{Ba}(\text{OH})_2$  phases [18, 34–38], unlike  $\text{BaCeO}_3$  and  $\text{BaCe}_{1-x}\text{Zr}_x\text{O}_3$  systems [29, 32, 39, 40]. Therefore, doped  $\text{BaZrO}_3$  is a suitable material for p-SOECs applications.

and will be the subject of this mini review to illustrate the proton conduction phenomena.  $\text{BaZrO}_3$  doped with Y, Yb, In, Sc, Gd, Nd, Sm, etc. have been extensively investigated as electrolytes that demonstrate considerable proton conductivity with optimized dopant element and concentration [5, 25, 26]. Several researchers have reported that the dopant and its concentration can considerably affect the proton conductivity of such materials [5, 25, 26]. Moreover, correlations between dopant atomic radius [25, 26] and electronegativity [41] with hydration energies and conductivities had been reported. Among doped  $\text{BaZrO}_3$  compounds, 20% Y-doped  $\text{BaZrO}_3$  has the highest conductivity to date [5, 25, 42]. However, there is a lack of comprehensive studies of doped  $\text{BaZrO}_3$  to characterize the differences between proton concentration and mobility with temperature and gas conditions. Meanwhile the pursuit of other possible compositions based on  $\text{BaZrO}_3$  perovskites is still ongoing to achieve higher conductivity.

This mini review will present the fundamental effects of defects location in material hydration and proton conduction. First, hydration thermodynamics for doped  $\text{BaZrO}_3$  materials and the effect of doping on

hydration and proton defect formation are reviewed. Second, proton localization in the lattice, particularly with respect to oxygen vacancies and dopant atoms, and the effect on proton concentration and mobility are presented in the context of defect associations and proton trapping phenomena. Finally, we present the implications of electronic conduction and strategies and future directions for further studies of proton-conducting materials.

**Thermodynamics of hydration in proton conductors**  
 The study of hydration thermodynamics is important for the characterization of new proton-conducting materials because hydration ability determines proton concentration under specific gas conditions and temperatures. Protons are incorporated into the material through the hydration of oxygen vacancies ( $\text{V}_\text{O}^\bullet$ ), as shown in equation (2). The oxygen vacancies are usually created by doping the B-site of the perovskite ( $\text{ABO}_3$ ) with a trivalent element (M) (equation (3)), and their concentration corresponds to half the dopant concentration. The hydration of oxygen vacancies in equation (2) is key as it determines the proton concentration ( $[\text{OH}_\text{O}]$ , % mol) of the material, which is a function of temperature, and under incomplete hydration, a function of water partial pressure ( $P_{\text{H}_2\text{O}}$ )



Favorable hydration thermodynamics can be used as a guide for proton conduction as it is related to proton concentration as a function of temperature. In this section, the basics of the hydration thermodynamics are reviewed, followed by a discussion about the incomplete hydration regime.

**Table1.**  $\Delta H_{\text{hyd}}$  and  $\Delta S_{\text{hyd}}$  of various doped BaZrO<sub>3</sub>.

Material	$\Delta H_{\text{hyd}}(\text{kJmol}^{-1})$	$\Delta S_{\text{hyd}}(\text{Jmol}^{-1}\text{K}^{-1})$	Reference
BaZr <sub>0.9</sub> Y <sub>0.1</sub> O <sub>3-δ</sub>	-79.4	-88.8	[5]
BaZr <sub>0.8</sub> Y <sub>0.2</sub> O <sub>3-δ</sub>	-93.3	-103.2	[5]
BaZr <sub>0.8</sub> Y <sub>0.2</sub> O <sub>3-δ</sub>	-22	-39	[50]
BaZr <sub>0.7</sub> Y <sub>0.3</sub> O <sub>3-δ</sub>	-26	-44	[50]
BaZr <sub>0.6</sub> Y <sub>0.4</sub> O <sub>3-δ</sub>	-26	-41	[50]
BaZr <sub>0.9</sub> Sc <sub>0.1</sub> O <sub>3-δ</sub>	-119.4	-124.9	[5]
BaZr <sub>0.8</sub> Sc <sub>0.2</sub> O <sub>3-δ</sub>	-96	-104	[51]
BaZr <sub>0.9</sub> Gd <sub>0.1</sub> O <sub>3-δ</sub>	-66.1	-85.9	[5]
BaZr <sub>0.9</sub> In <sub>0.1</sub> O <sub>3-δ</sub>	-66.6	-90.2	[5]
BaZr <sub>0.9</sub> In <sub>0.1</sub> O <sub>3-δ</sub>	-67	-90	[52]
BaZr <sub>0.5</sub> In <sub>0.5</sub> O <sub>3-δ</sub>	-60	-95	[52]
BaZr <sub>0.25</sub> In <sub>0.75</sub> O <sub>3-δ</sub>	-74	-109	[52]

The thermodynamics of the hydration reaction, equation (2), determines the proton concentration of the material as a function of temperature. The formation of the proton defect is governed by the equilibrium constant of the hydration reaction ( $K_{\text{hyd}}$ ), equation (4)

$$[\text{OH}_\text{O}^\bullet]^2$$

$$\frac{K_{\text{hyd}}}{P} = \frac{[\text{V}^*][\text{O}^\bullet]}{[\text{H}_2\text{O}]} \quad (4)$$

$H_2O \rightleftharpoons O^\bullet$   
 $K_{\text{hyd}}$  is then related to the Gibbs free energy of hydration ( $\Delta G_{\text{hyd}}$ ) according to equation (5), while  $\Delta G_{\text{hyd}}$  is related to the enthalpy ( $\Delta H_{\text{hyd}}$ ) and entropy ( $\Delta S_{\text{hyd}}$ ) of hydration according to equation (6). Therefore,  $\Delta H_{\text{hyd}}$  and  $\Delta S_{\text{hyd}}$  can be calculated from knowing  $K_{\text{hyd}}$  as a function of temperature through the Van't Hoff equation, as shown in equation (7)

$$\begin{aligned} \Delta G_{\text{hyd}} &= -RT \ln K_{\text{hyd}} \\ \Delta G_{\text{hyd}} &= \Delta H_{\text{hyd}} - T\Delta S_{\text{hyd}} \end{aligned}$$

$$\frac{\ln K_{\text{hyd}}}{\Delta H_{\text{hyd}}} = \frac{\Delta S_{\text{hyd}}}{T} + C$$

Favorable hydration thermodynamics is often characterized by a highly exothermic  $\Delta H_{\text{hyd}}$ , a less negative  $\Delta S_{\text{hyd}}$ , and a negative  $\Delta G_{\text{hyd}}$ . Materials with more exothermic heats of hydration favor higher degrees of hydration at a given temperature. The entropic impact of hydration is related to lattice ordering due to proton incorporation [5], which results in lattice expansion upon hydration and includes configuration and vibrational contributions [44]. In general, a less negative value of  $\Delta S_{\text{hyd}}$  usually results in greater retention of protons

at higher temperatures [44,45]. Studies of doped BaZrO<sub>3</sub> hydration thermodynamics have correlated  $\Delta H_{\text{hyd}}$  with the electronegativity of the dopant and tolerance factor of the material [41,46,47]. As the tolerance factor and electronegativity of the dopant decreases,  $\Delta H_{\text{hyd}}$  tends to be more exothermic

[47]. The effects of the dopant and its concentration on  $\Delta H_{\text{hyd}}$  and  $\Delta S_{\text{hyd}}$  are summarized in Table 1. The values of  $\Delta H_{\text{hyd}}$  and  $\Delta S_{\text{hyd}}$  are dependent on the dopant, decreasing in hydration energy as follows: Gd > In > Y, with Sc-doped BaZrO<sub>3</sub> exhibiting the most favorable  $\Delta H_{\text{hyd}}$ . However,  $\Delta H_{\text{hyd}}$  and  $\Delta S_{\text{hyd}}$  do not show any clear dependence on dopant concentration. Differences in the values of the hydration energy between references for a same material correspond to possible non-linear hydration isobars in all temperature ranges ascribed to defect interactions [48,49] or to the formation of ionic species [50].

An important feature that results from studying the hydration of a material is the characterization of proton concentration with temperature. The hydration limit of doped BaZrO<sub>3</sub> frequently corresponds to the theoretical level of the dopant concentration [M]. Proton concentration as a function of temperature has been reported for numerous doped BaZrO<sub>3</sub> where the proton concentration reaches a maximum value at a low temperature and follows a decreasing trend with increasing temperature, as shown in figure 1(a). Proton concentration is normally studied through thermogravimetric analysis by correlating the weight increase from water uptake to the proton concentration, usually while studying hydration thermodynamics. Nuclear magnetic resonance (NMR) [53] has also been used to quantify the proton concentration. The application of these materials for p-SOECs requires operating temperatures in the range of 400 °C–600 °C, i.e. in the incomplete hydration regime, as seen in figures 1(a) and (b). A thoughtful characterization of the incomplete

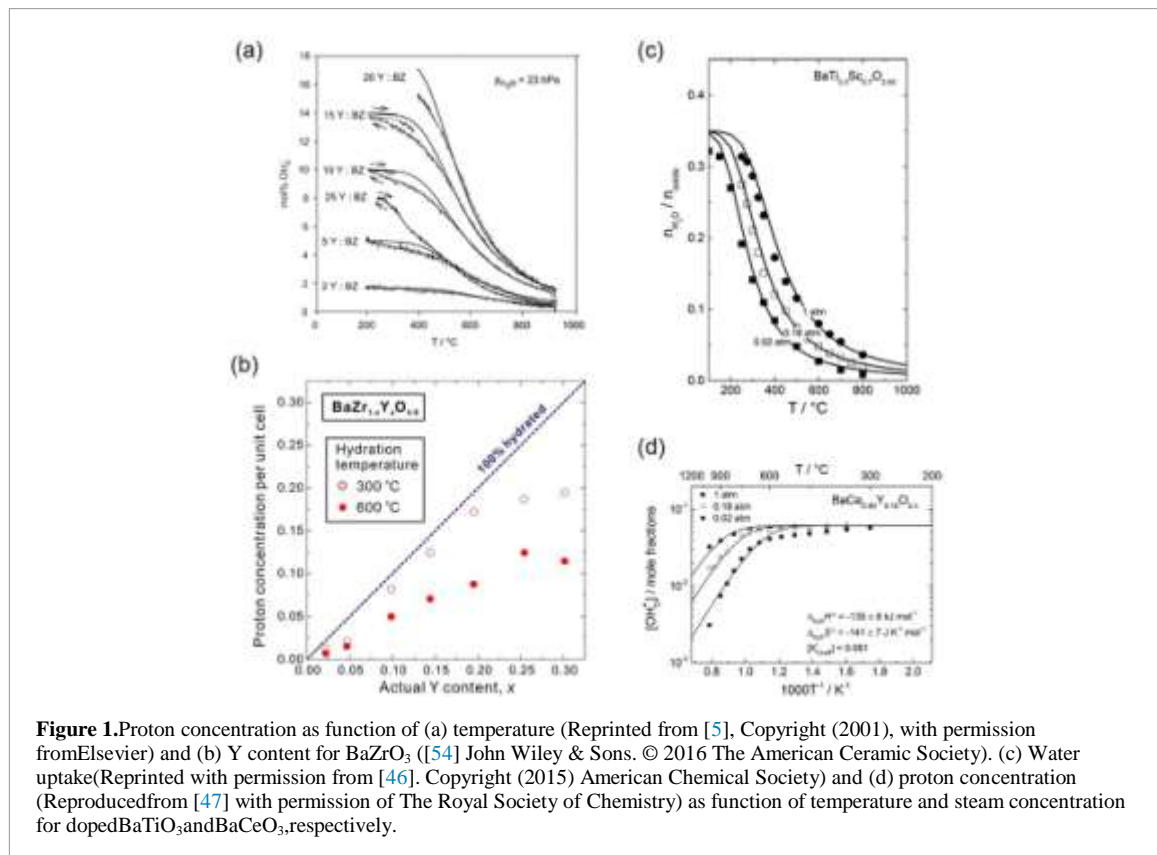


**Figure 1.** Proton concentration as function of (a) temperature (Reprinted from [5], Copyright (2001), with permission from Elsevier) and (b) Y content for BaZrO<sub>3</sub> ([54] John Wiley & Sons. © 2016 The American Ceramic Society). (c) Water uptake (Reprinted with permission from [46]. Copyright (2015) American Chemical Society) and (d) proton concentration (Reproduced from [47] with permission of The Royal Society of Chemistry) as function of temperature and steam concentration for doped BaTiO<sub>3</sub> and BaCeO<sub>3</sub>, respectively.

hydration regime becomes essential to determine optimum doping concentrations. However, there are not many studies exploring this relationship. Moreover, in the incomplete hydration regime, proton concentration is a function of steam concentration [46, 47], as seen in figures 1(c) and (d) for other perovskites. Figures 1(c) and (d) suggest that proton concentration increases as steam

concentration increases, although the effect is more significant in the low steam concentration region. Future studies on the proton concentration in doped BaZrO<sub>3</sub> as a function of steam concentration and temperature should reveal the dynamic of material hydration.

It is worth pointing out that BaZrO<sub>3</sub>-based electrolytes are refractory materials that require high sintering temperatures. To reduce the sintering temperature and improve densification, sintering aids (NiO [55–57], ZnO [58–61], CuO [55, 62], CaO [63], BaO–B<sub>2</sub>O<sub>3</sub> [64], BaY<sub>2</sub>NiO<sub>5</sub> [65], etc.) have been used to facilitate densification by introducing a liquid phase for grain growth [66]. However, recent studies have shown that sintering aids have negative impact on the proton concentration [67–69], thus reducing conductivity. In addition, the sintering aids favor

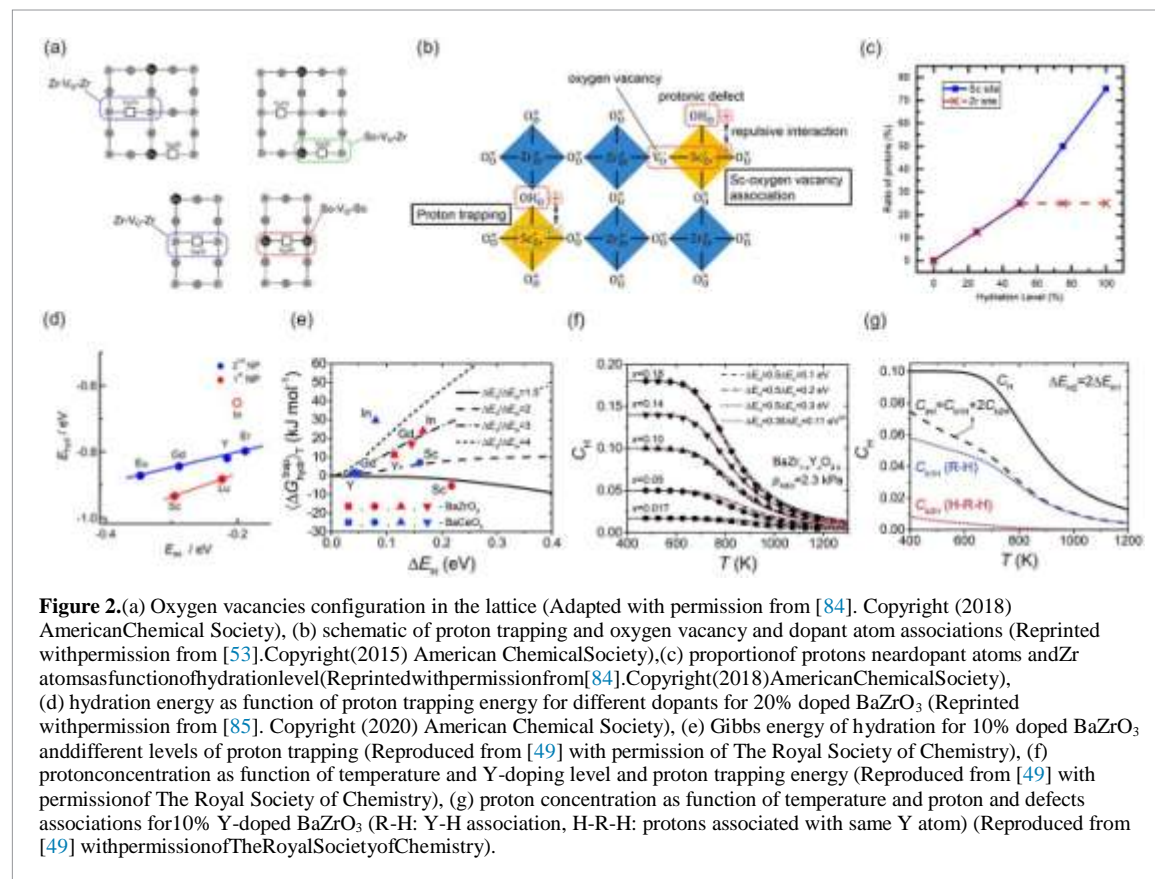
orthodetrimental formation of Ba-vacancies [67, 68] and the formation of undesired secondary phases in Y-doped BaZrO<sub>3</sub> [69–71]. Therefore, it is important to minimize the use of sintering aids or adopt other strategies for the material densification to suppress the impact of sintering aids on the conductivity.

Based on  $K_{hyd}$  and the hydration energies, lower temperatures and higher steam concentrations are favorable for the hydration of oxygen vacancies. A higher concentration of oxygen vacancies increases the proton concentration. The doping of the Zr-site is the most common strategy to create oxygen vacancies but Ba-site doping has also been explored [72–74]. The oxidizing character of the steam carrier gas is another important factor to consider during hydration as the oxidation of oxygen vacancies at certain experimental conditions [75, 76] could decrease the effective concentration of oxygen vacancies that can be hydrated. The effects of oxygen vacancies and dopant atoms in the material hydration will be discussed in the following sections.

#### Effect of oxygen vacancies and defects association on hydration and proton concentration

The location of oxygen vacancies and the extent of defect association are a representation of the chemical environment differences caused by dopants as

nd their concentration. These differences manifest in the hydration energies and, consequently, in proton concentration. While it has been suggested that oxygen



vacancies tend to form in the vicinity of dopant atoms [53, 77], different configurations of oxygen vacancies can exist. Several workshave successfully proved the localization of oxygen vacancies and protons at different configurations in doped BaZrO<sub>3</sub> by using specialized techniques such as neutron spin-echo [78], x-ray absorption spectroscopy [52], quasielastic neutron scattering [79, 80], Fourier transform infrared spectroscopy [81–83], and NMR [53, 84]. Some of those configurations correspond to oxygen vacancies in between Zr atoms (Zr–V–Zr), between a Zr atom and a dopant atom (Zr–V–M), and in between dopant atoms (M–V–M) [84], as represented schematically in figure 2(a). The distribution of such configurations can be a function of the dopant atom and its concentration as a result of charge compensation during the formation of oxygen vacancies (equation (3)). On the other hand, positively charged protons and oxygen vacancies can associate with negatively charged dopant atoms [53], as seen in figure 2(b), for which the extent of such associations is a function of the dopant [77]. In this section, the oxygen

vacancy location and defect associations will be used to discuss the hydration energy and proton concentration of doped BaZrO<sub>3</sub>. The location of oxygen vacancies before their hydration has an impact on hydration energy. Consequently, oxygen vacancies near dopant atoms can be part of defect associations that can modify the hydration thermodynamics and the treatment of experimental data about the material hydration [48, 49]. Computational works have shown that the hydration energy of each configuration is different, suggesting that the experimental hydration energies are an average of all the different hydration energies for all the oxygen vacancy configurations [84, 86]. Additionally, some attempts to link the extent of hydration to the location of oxygen vacancies have been made by relating the stability of oxygen vacancies with their hydration abilities [84]. For example, density functional theory (DFT) of Sc-doped BaZrO<sub>3</sub> showed that the stability of oxygen vacancies depends on its location, being more stable near Sc atoms in comparison with oxygen vacancies near Zr atoms [84]. Consequently, the less stable oxygen vacancies are

easier to hydrate than the more stable oxygen vacancies [84, 87]. This is significant as the hydration of some oxygen vacancies could result in protons in proton trapping positions. However, a Sc-NMR study on the hydration of Sc-doped BaZrO<sub>3</sub> revealed that at low proton concentrations, i.e. low material hydration due to high temperature, the protons were located equally near the Sc and Zr atoms [53, 84]. But as the proton concentration increased, i.e. a material hydration increased by low temperatures, most of the protons were located near Sc [53, 84], as seen in figure 2(c).

The association of a proton with a dopant atom is referred to as proton trapping. DFT studies have correlated hydration energy with proton trapping energy for different dopants in BaZrO<sub>3</sub>. The results suggested that high proton trapping energy led to more exothermic hydration energies [85], as shown in figure 2(d). However, another DFT study suggested that proton trapping can enhance or inhibit the hydration of the material [49], as can be observed from figure 2(e) where the Gibbs free energy of hydration is presented as a function of the proton association energies. Such boundaries depend on the dopant and its concentration, as well as the trapping energy for the proton and for the oxygen vacancies with the dopant [49]. As shown in figures 2(d) and (e), as defect associations affect hydration equilibrium, failing to include these associations in the data analysis of hydration measurements could affect the calculation of proton concentrations [48, 49, 85, 88]. As seen in figure 2(f), at higher doping concentration for Y-doped BaZrO<sub>3</sub>, the proton concentration does not reach theoretical values at the low temperature region [49]. Additionally, the overall proton concentration could be divided between the un-associated protons and trapped protons [49], as seen in figure 2(g). The effect of trapped protons and unassociated protons on proton conduction will be reviewed next. Nonetheless, the complexity added by defect association on proton concentration must be understood as the search for the optimum dopant and doping concentration of BaZrO<sub>3</sub> continues.

### Proton conduction in solid oxides

It is well recognized that protons diffuse through solid oxides by the Grotthuss mechanism. Proton diffusion involves the reorientation of a proton towards a neighboring oxygen atom and the jump of the proton towards the neighboring oxygen atom [41, 89], as shown in figure 3(a). The proton jump step is mostly considered as the rate limiting step [41, 89]. Due to the nature of the Grotthuss mechanism,

H bonds become important in the understanding of proton conduction in perovskites. The O-H bond can be stretched, shortened, and reoriented due to the atoms around it, changing in strength accordingly [82]. Normally, when the O-H bond is stronger, the rate of reorientation decreases and proton transfer increases [82]. Oxygen vacancies and dopant atoms can modify the O-H bond strength. For example, it was reported that as the oxygen vacancies and dopant atoms influence a repulsive and attractive force around the proton due to their positive and negative charge, respectively, the proton tilt towards a neighboring oxygen and hence stronger O-

H bonds are created [82]. The overall effect is observed in the increase in the proton jump step at the expense of slowing the reorientation step [41, 82], modifying the activation energy for proton diffusion. Moreover, the B-H interaction can also contribute to the activation energy of proton diffusion as the repulsive interaction between a proton and the host atom B inhibits the formation of a linear O-H bond, resulting in an increase of activation energy for proton transfer [41, 45, 90]. The B-H interaction can be modified by doping resulting in changes in the basicity of the oxygen atoms and in the activation energy for proton diffusion [41, 90].

Proton diffusion from the surface to the bulk of the material could represent an important energy barrier, as suggested by DFT studies in proton conductor oxides [87, 91]. As seen in figure 3(b), the energy barriers for the initial proton jump (I and T in figure 3(b)) are higher than the energy barrier for proton jumps away from the surface [91]. Additionally, the study of the material surface and its space charge region is relevant for the study of the hydration process [87, 92]. Proton diffusion into the bulk requires the counter diffusion of oxygen vacancies from the bulk to the surface, and therefore, the predicted depletion or segregation of oxygen vacancies (figure 3(c)) could increase the energy barriers for proton diffusion from the surface to the bulk of the material. Thorough studies about the energy barriers for proton diffusion from the surface to the bulk in doped BaZrO<sub>3</sub> could help explain the differences in conductivity observed experimentally for different dopants.

Proton conductivity is proportional to proton mobility ( $\mu_{OH} \cdot m^2 V^{-1} s^{-1}$ ) and proton diffusivity ( $D_{OH} \cdot m^2 s^{-1}$ ) according to equations (8) and (9), respectively,

$$\sigma_{OH} = \frac{\mu_{OH} \cdot D_{OH}}{kT}$$

$$\frac{z_{OH} F [OH_o] \mu_{OH}}{V_M}$$

(8)

$$\sigma_{OH} = \frac{z^2 f^2 [OH_o] D_{OH}}{RT}$$

where  $z_{OH}$  is the proton charge,  $F$  is the Faraday constant,  $V_M$  is the molar volume of the ceramic ( $m^3 mol^{-1}$ ), and  $R$  is the gas constant.  $D_{OH}$  and  $\mu_{OH}$  are related through the Nernst–Einstein equation, as shown in equation (10)

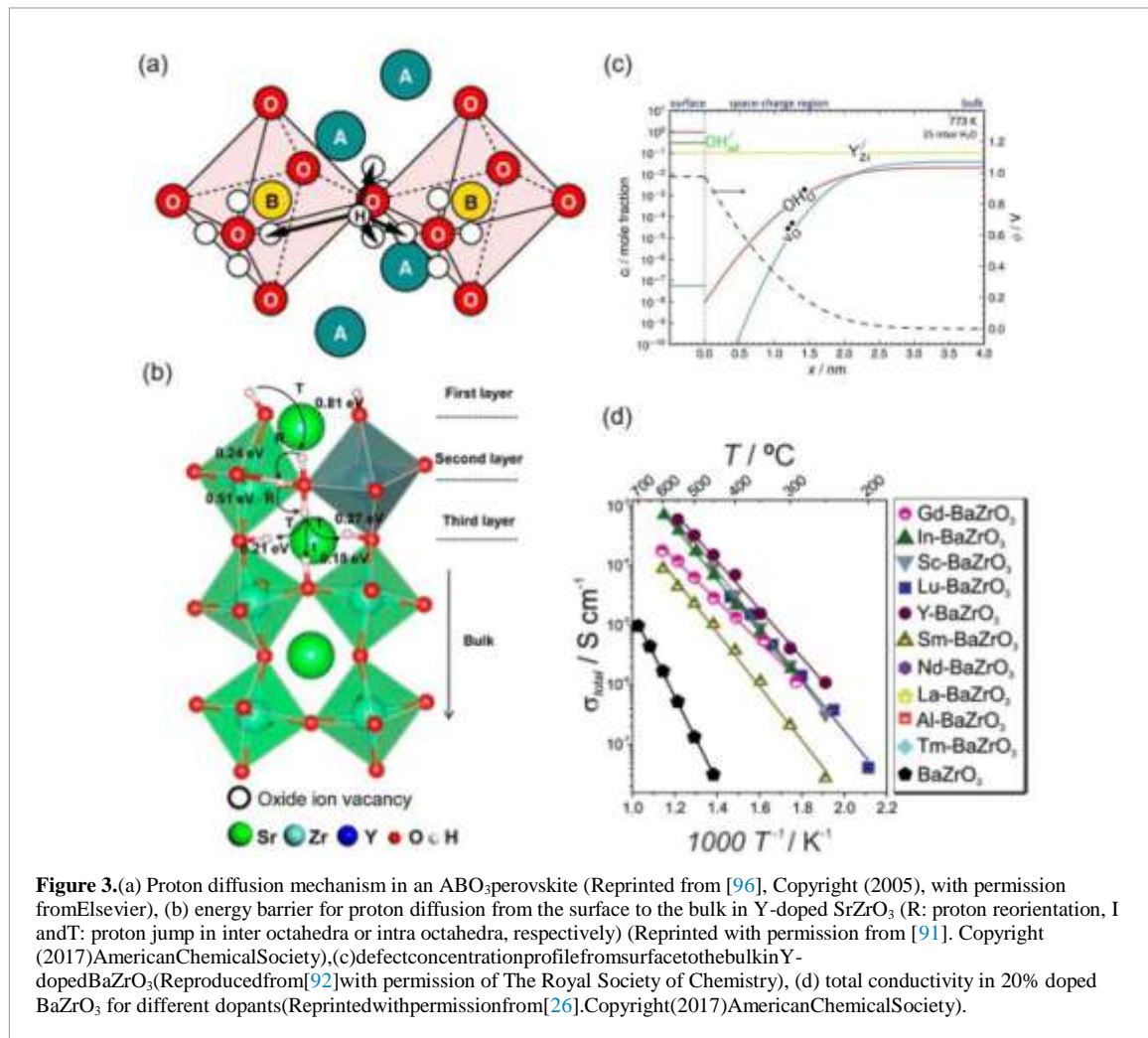


**Table 2.** Activation energy,  $E_a$ , and total conductivity in wet reducing or inert gas,  $\sigma_{\text{total}}$ , at  $600^\circ\text{C}$  of various doped  $\text{BaZrO}_3$ .

Material	$E_a$ (eV)	Reference	$\sigma_{\text{total}}$ ( $\text{Scm}^{-1}$ )	Reference
$\text{BaZr}_{0.9}\text{Y}_{0.1}\text{O}_{3-\delta}$	0.43	[5]	—	
$\text{BaZr}_{0.8}\text{Y}_{0.2}\text{O}_{3-\delta}$	0.48	[5]	0.004 0.0125	[93,94]
$\text{BaZr}_{0.7}\text{Y}_{0.3}\text{O}_{3-\delta}$	—		0.0011	[93]
$\text{BaZr}_{0.6}\text{Y}_{0.4}\text{O}_{3-\delta}$	—		0.0007	[93]
$\text{BaZr}_{0.9}\text{Sc}_{0.1}\text{O}_{3-\delta}$	0.50	[5]	—	
$\text{BaZr}_{0.8}\text{Sc}_{0.2}\text{O}_{3-\delta}$	0.50	[51]	0.005	[51]
$\text{BaZr}_{0.9}\text{Gd}_{0.1}\text{O}_{3-\delta}$	0.47	[5]	—	
$\text{BaZr}_{0.8}\text{Gd}_{0.2}\text{O}_{3-\delta}$	—		0.0002	[26]
$\text{BaZr}_{0.9}\text{In}_{0.1}\text{O}_{3-\delta}$	0.48	[5]	—	
$\text{BaZr}_{0.8}\text{In}_{0.2}\text{O}_{3-\delta}$	—		0.0006	[95]
$\text{BaZr}_{0.5}\text{In}_{0.5}\text{O}_{3-\delta}$	0.62	[52]	—	
$\text{BaZr}_{0.25}\text{In}_{0.75}\text{O}_{3-\delta}$	0.40	[52]	—	
$\text{BaZr}_{0.8}\text{Sm}_{0.2}\text{O}_{3-\delta}$	—		0.00009	[26]

$$\begin{aligned} \text{DOH}_\bullet &= \\ \mu\text{OH}_\bullet &= \\ \text{RT} &= \\ &= \\ z_{\text{OH}}\text{O}^\bullet &= \text{F} \end{aligned}$$

.(10)

The activation energies (see equation (1)) obtained from conductivity measurements are frequently reported and table 2 shows the activation energy of various doped BaZrO<sub>3</sub> with all materials in the range of 0.4–0.6 eV. As seen in table 2, the choice of dopant and dopant concentration can modify the activation energy for proton conduction. For example, the activation energies from the same study at 10% doping are 0.43 eV for Y, 0.50 eV for Sc, 0.48 eV for In, and 0.47 eV for Gd [5]. Additionally, the effect of the dopant choice on proton diffusivity can be appreciated in figure 3(d) where the conductivity differences are about two orders of magnitude for different dopants [26] and on table 2 where representative conductivities at 600 °C are shown.

Consequently, understanding the proton conduction phenomena and how different materials and material doping can modify proton conduction is central to advancing proton-conducting materials research. It is worth mentioning that the conduction of oxygen ions (or V<sub>O</sub><sup>•</sup>) can also exist in proton-conducting oxides. Some studies have shown no oxygen ion conduction at low oxygen partial pressures and dry conditions [97–99] at increased temperature, usually above 700 °C [100, 101]. This mixed proton and oxygen ion conduction in the electrolyte has been reported to be beneficial for solid oxide cells. For example, studies have shown an increase of efficiencies in fuel cell operation [23, 102, 103] and, when steam is added to the electrodes in electrolysis operation, an increase on the hydrogen production due to the simultaneous water electrolysis on both electrodes [19]. Nevertheless, it should be considered that the gain of additional oxygen ion conduction does not diminish the proton conductivity due to the conditions necessary for the oxygen ion conduction.

#### Proton trapping and its effect on proton transport

Proton trapping reduces the proton mobility and is manifested in the increase of activation energy for proton conduction at lower temperatures [88]. At low temperatures, the protons do not have enough energy to move from the trapping positions, hence the nonlinearity of the activation energy seen for this temperature range. This phenomenon has been receiving increased attention as some material applications

are operating at temperatures that could fall under the proton trapping regime. Evidence of proton trapping requires the probing of proton position near dopant atoms. However, computational methods have predicted proton trapping conditions. Figure 4(a) shows a schematic representation of proton binding energies for Y-

doped BaZrO<sub>3</sub> for different proton configurations, where the proton configuration in between two Y atoms has the highest binding energy [104].

In section 3 it was pointed out that increasing doping concentration increases proton trapping. Nonetheless, computational work has found that as proton trapping increases due to higher

proton concentration there is a point where the trapped protons prevent other protons from being trapped and percolation channels form due to the overlap of trapping zones, and hence the proton mobility increases again [105, 106]. However, the doping concentration for the formation of percolation channels could be dependent on the dopant element. Additionally, proton-proton interactions could have a negative effect on proton mobility with increasing proton concentration due to their repulsive

interaction [106]. However, in 20% Y-doped BaZrO<sub>3</sub>, such negative interactions are not dominant, and instead, the trapped protons enhance the proton mobility of the free protons by filling the trapping positions [106].

Defect associations also have an effect on proton trapping. Oxygen vacancies and dopant atoms can form an association that could prevent the trapping effect (figure 2(b)) [53, 77]. On the other hand, the dopant-

dopant association can modify transport properties of the material and could enhance proton trapping [107]. A DFT study looking at Y-

Y defect associations and their effect on proton trapping on Y-

doped BaZrO<sub>3</sub> suggested that a triangular configuration of Y associations is responsible for the proton trapping phenomena observed in Y-doped BaZrO<sub>3</sub> [107], as shown in figure 4(b). For Y-doped BaZrO<sub>3</sub>, studies have suggested that the Y-Y associations increase with doping concentration [107, 108].

Finally, doping concentration and dopant element choice yield varied effects on proton trapping.

Figure 4(c) shows conductivity as a function of Y doping concentration, and it can be observed that there is an optimum concentration where conductivity is maximized [107]. However, the ideal doping level for different elements may not necessarily be the same. Figure 4(d) shows proton

conductivity as a function of proton trapping for different dopant elements for  $\text{BaZrO}_3$ , where the correlation shows that for favorable proton trapping energy the proton conductivity decreases [85]. Amid all these transport phenomena, the analysis of proton conductivity at specific operating conditions should be carefully considered and a balance between doping concentration, proton concentration, and proton mobility is essential.

#### Electronic conduction in solid oxides

In addition to the proton conduction of  $\text{BaZrO}_3$ ,

based electrolytes, electronic defects such as hole defects ( $\text{h}^+$ ) are formed by the oxidation of oxygen vacancies according to equation (11). Hole defects can be considered a main charge carrier under certain experimental conditions, typically under high oxygen partial pressures and dry conditions [2, 99, 109]. Therefore, the implications of electronic conduction in solid oxides are briefly discussed

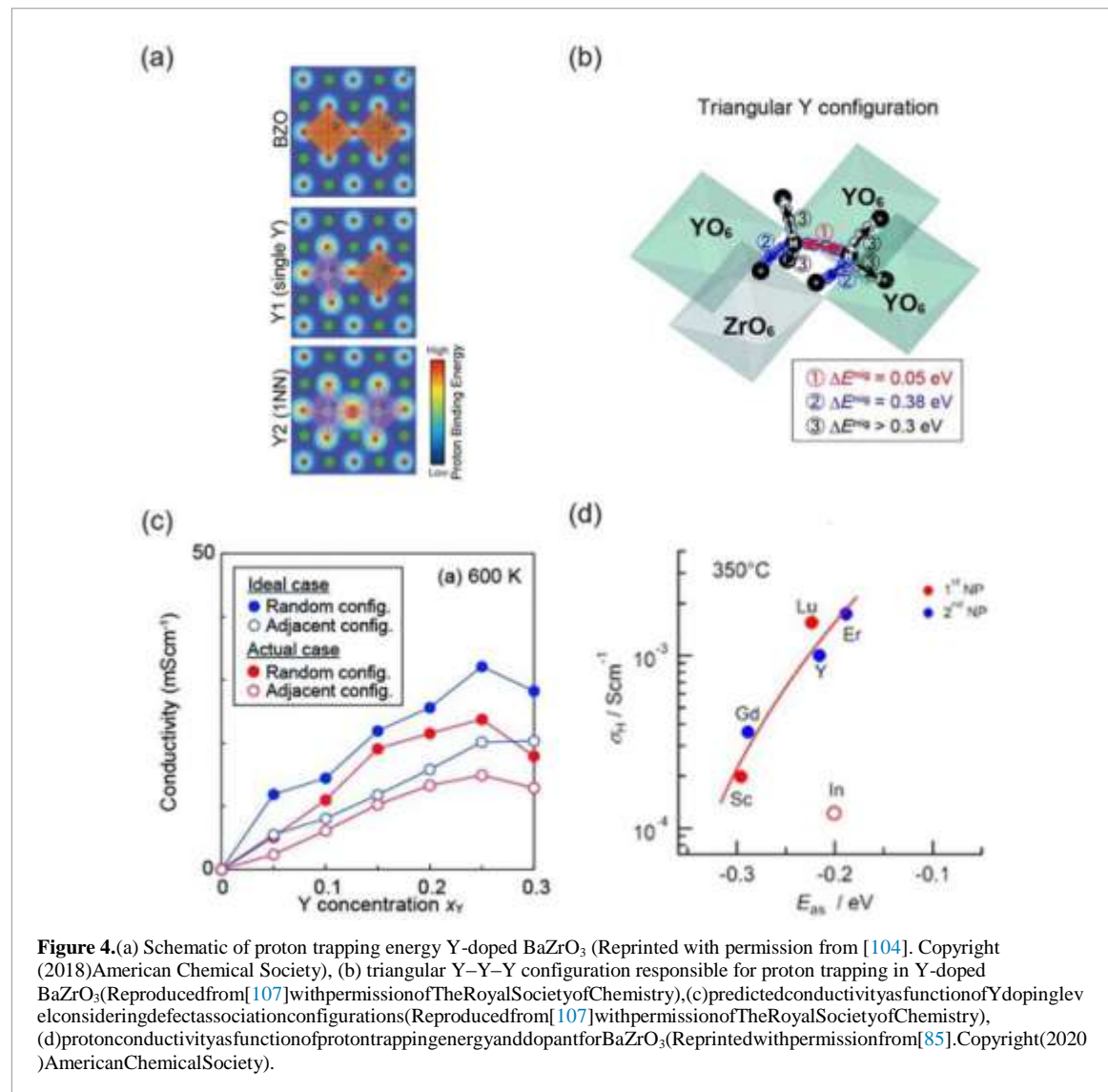
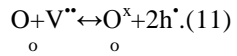


**Figure 4.**(a) Schematic of proton trapping energy Y-doped  $\text{BaZrO}_3$  (Reprinted with permission from [104]. Copyright (2018) American Chemical Society), (b) triangular  $\text{Y}-\text{Y}-\text{Y}$  configuration responsible for proton trapping in Y-doped  $\text{BaZrO}_3$  (Reproduced from [107] with permission of The Royal Society of Chemistry), (c) predicted conductivity as a function of Y doping level considering defect association configurations (Reproduced from [107] with permission of The Royal Society of Chemistry), (d) proton conductivity as a function of proton trapping energy and dopant for  $\text{BaZrO}_3$  (Reprinted with permission from [85]. Copyright (2020) American Chemical Society).

The main concern for electronic conduction is related to the electronic leakage in p-SOECs, where such leakage decreases the Faradaic efficiency [10, 17, 21]. Several advances have been made towards the understanding of hole conduction, such as the development

of defect chemistry and transport models that highlight the conditions benefitting hole formation and conduction [17, 21, 110–113].

The effect of electronic defects on material hydration has also been studied. Theoretical models

has suggested that electronic defects have the potential to modify the material hydration by the formation of deep acceptor states [75, 76]. Additionally, the nonlinearity of the hydration isobars has been attributed to electronic defect formation [50]. Experimental studies have also shown a two-fold proton diffusion from the surface to the bulk of the material under high temperatures and high oxygen partial pressure suggesting that the hole conduction decouples the diffusion of protons and oxygen vacancies [114, 115]. Thus, the dominance of oxygen vacancy hydration over oxidation is critical to the understanding of material hydration and subsequent proton and electronic conduction in solid oxides.

### Concluding remarks and prospects

As discussed in this mini review, attention must be given not only to the choice of dopant but also to its concentration. High doping concentrations can be strategic for improving proton concentration, as presented by a recent work in Sc-doped BaZrO<sub>3</sub> [51]. While the effect of percolation channels for proton conduction and different defect associations can be further explored for high doping materials, some problematic aspects of high concentration of dopants such as phase stability and sinterability should be considered.

A comprehensive study of the effects of the gas condition on proton conduction in these materials is necessary. The underlying mechanism responsible for proton conductivity differences as a function of the gas condition remains unclear for the most part, especially when it comes to how proton conduction is affected by high steam concentrations and highly oxidizing atmospheres. Hence, the effect of gas conditions on the thermodynamics and transport phenomena should be thoroughly considered.

Finally, coupling advanced characterization techniques with simulations could enhance the understanding of proton conduction mechanisms, particularly proton formation and diffusion. By inputting proton conduction parameters, the developed models will be able to predict relevant p-SOECs properties such as proton current density and efficiency as a function of operating conditions.

### Data availability statement

No new data were created or analysed in this study.

### REFERENCES

- [1] Iwahara H, Esaka T, Uchida H and Maeda N 1981 Proton conduction in sintered oxides and application to steam electrolysis for hydrogen production Solid State Ion. **3/4** 359–63
- [2] Uchida H, Maeda N and Iwahara H 1983 Relation between proton and hole conduction in SrCeO<sub>3</sub>-based solid electrolytes under water-containing atmospheres at high temperatures Solid State Ion. **11** 117–24
- [3] Haugsrud R and Norby T 2006 Proton conductivity in rare-earth ortho-niobates and ortho-tantalates Nat. Mater. **5** 193–6
- [4] Fop S, McCombie K S, Wildman E J, Skakle J M S, Irvine J T S, Connor P A, Savaniu C, Ritter C and McMullan A C 2020 High oxide ion and proton conductivity in a disordered hexagonal perovskite Nat. Mater. **19** 752–7
- [5] Kreuer K D, Adams S, Munch W, Fuchs A, Klock U and Maier J 2001 Proton conducting alkali and earth zirconates and titanates for high drain electrical applications Solid State Ion. **145** 295–306
- [6] Ding D, Zhang Y, Wu W, Chen D, Liu M and He T 2018 A novel low-thermal-budget approach for the co-production of ethylene and hydrogen via the electrochemical non-oxidative deprotonation of ethane Energy Environ. Sci. **11** 1710–6
- [7] Iwahara H, Asakura Y, Katahira K and Tanaka M 2004 Prospect of hydrogen technology using proton-conducting ceramics Solid State Ion. **168** 299–310
- [8] Li M, Hua B, Wang L, Sugar J D, Wu W, Ding Y, Li J and Ding D 2021 Switching of metal–oxygen hybridization for selective CO<sub>2</sub> electrohydrogenation under mild temperature and pressure Nat. Catal. **4** 274–83
- [9] Iwahara H 1995 Technological challenges in the application of proton conducting ceramics Solid State Ion. **77** 289–98
- [10] Duan C et al. 2018 Highly durable, coking and sulfur tolerant, fuel-flexible protonic ceramic fuel cells Nature **557** 17–22
- [11] Wu W, Ding H, Zhang Y, Ding Y, Katiyar P, Majumdar P K, He T and Ding D 2018 3D self-architected steam electrode enabled efficient and durable hydrogen production in a proton-conducting solid oxide electrolysis cell at temperatures lower than 600 °C Adv. Sci. **5** 1800360
- [12] Irvine J T S, Neagu D, Verbraeken M C, Chatzichristodoulou C, Graves C and Mogensen M B 2016 Evolution of the electrochemical interface in high-temperature fuel cells and electrolyzers Nat. Energy **11** 5014
- [13] Zhan Z, Bierschenk D M, Cronin J S and Barnett S A 2011 A reduced temperature solid oxide fuel cell with nanostructured anodes Energy Environ. Sci. **4** 274–83

- ci.43951–4
- [14] WuJ,JohnsonCD,GemmenRSandLiuX2009The performanceofsolidoxidefuelcellswithMn–Coelectroplatedinterconnectascathodecurrent collectorJ.PowerSources**189**1106–13
- [15] TaoSW,IrvineJTSandKilnerJA2005An efficient solidoxidefuelcellbaseduponsingle-phaseperovskitesAdv.Mater.**17**1734–7
- [16] DuanC,KeeR,ZhuH,SullivanN,ZhuL,BianL,JenningsDandO’HayreR2019Highlyefficient reversibleprotionicceramicelectrochemicalcell sforpowergenerationandfuelproductionNat.Energy**4**230–40
- [17] ChoiS,DavenportTCandHaileSM2019Proton icceramicelectrochemicalcellsforhydrogenpr oductionandelectricitygeneration:exceptional reversibility,stability, anddemonstratedfaradai cefficiencyEnergyEnviron.Sci.**12**206–15
- [18] DuanC,TongJ,ShangM,NikodemskiS,Sanders M,RicoteS,AlmansooriAandOHayreR2015Rea dilyprocessedprotionicceramicfuelcellswithhi g hperformanceatlowtemperaturesScience**349** 321–6
- [19] KimJ,JunA,GwonO,YooS,LiuM,ShinJ,LimT- HandKimG2018Hybrid- solidoxideelectrolysiscell:anewstrategyforeffic ienthydrogenproductionNanoEnergy**44**121– 6
- [20] DipponM,BabiniecSM,DingH,RicoteSandSu llivanNP2016Exploringelectronicconduction throughBaCe<sub>x</sub>Zr<sub>0.9-x</sub>Y<sub>0.1</sub>O<sub>3-d</sub>proton- conductingceramicsSolidStateIon.**286**117– 21
- [21] VøllestadE,StrandbakkeR,TarachM,Catalan- MartinezD,FontaineML,BeeaffD,ClarkDR,S erraJManNorbyT2019 Mixed protonandelectronconductingdoubleperovskit eanodesforstableandefficienttubularprotone ramicelectrolyzersNat. Mater.**18**752–9
- [22] DingHetal2020Self- sustainableprotionicceramicelectrochemicalc ellsusingatripleconductingelectrodeforhydro genandpowerproductionNat.Commun.**11**190 7
- [23] YangL,WangS,BlinnK,LiuM,LiuZ,ChengZa ndLiuM2009Enhancedsulfurandcokingtolera nceofamixedionconductorforSOFCs:BaZr<sub>0.1</sub> Ce<sub>0.7</sub>Y<sub>0.2-x</sub>Yb<sub>x</sub>O<sub>3-d</sub>Science**326**126–9
- [24] ChoiS,KucharczykCJ,LiangY,ZhangX,Takeuci hil,JiH- IandHaileSM2018Exceptionalpowerdensityand stabilityat intermediatemtemperaturesinprotionicceramicfuelcell sNat.Energy**3**202–10
- [25] HanD,ShinodaK,SatoS,MajimaMandUdaT2 015Correlationbetweenelectroconductiveand structuralpropertiesofprotonconductiveaccep
- tor- dopedbariumzirconateJ.Mater.Chem.A**3**124 3–50
- [26] GilardiE,FabbriE,BiL,RuppJLM,LippertT,Perg olesiDandTraversaE2017Effectofdopant- hostonicradiimismatchonacceptor- dopedbariumzirconatemicrostructureandprot onconductivityJ.Phys.Chem.C**121**9739–47
- [27] XieK,YanR,ChenX,DongD,WangS,LiuXandM engG2009AnewstableBaCeO<sub>3-</sub> basedprotonconductorforintermediate- temperaturesolidoxidefuelcellsJ.AlloysCom pd.**47**2551–5
- [28] MurphyR,ZhouY,ZhangL,SouleL,ZhangW,Ch enYandLiuM2020Anewfamilyofproton- conductingelectrolytesforreversiblesolidoxide cells:BaHf<sub>x</sub>Ce<sub>0.8-x</sub>Y<sub>0.1</sub>Yb<sub>0.1</sub>O<sub>3-d</sub>Adv.Funct.M ater.**30**2002265
- [29] ZhangY,XieD,ChiB,PuJ,LiJandYanD2019B asicpropertiesofprotonconductorBaZr<sub>0.1</sub>Ce<sub>0.7</sub> Y<sub>0.1</sub>Yb<sub>0.1</sub>O<sub>3-d</sub>(BZCYYb)materialAsia-Pac.J. Chem.Eng. **14**e2322
- [30] Qian J, Sun W, Shi Z, Tao Z and Liu W 2015 Chemically stable BaZr<sub>0.7</sub>Pr<sub>0.1</sub>Y<sub>0.2</sub>O<sub>3-d</sub>- BaCe<sub>0.8</sub>Y<sub>0.2</sub>O<sub>3-d</sub>bilayer electrolyte forintermediatemtemperaturesolidoxidefuelcel lsElectrochim.Acta**151**497–501
- [31] YooYandLimN2013Performanceandstability ofprotonconductingsolidoxidefuelcellsbased onyttrium-dopedbariumcerate-zirconatethin- filmelectrolyteJ.PowerSources**229**48–57
- [32] ReddyGSandBauriR2016YandIn- dopedBaCeO<sub>3-</sub> BaZrO<sub>3</sub>solidsolutions:chemicallystableanda silysinterableprotonconductingoxidesJ.Alloy sCompd.**688**1039–46
- [33] MedvedevD,LyagaevaJ,PlaksinS,DeminAandT siakarasP2015SulfurandcarbontoleranceofBaC eO<sub>3</sub>–BaZrO<sub>3</sub>proton- conductingmaterialsJ.PowerSources**273**716– 23
- [34] BiL,ShafiSPandTraversaE2015Y- dopedBaZrO<sub>3</sub>aschemicallystableelectrolytef orproto- conductingsolidoxideelectrolysiscells(SOEC s)J.Mater.Chem.A**3**5815–9
- [35] FabbriE,PergolesiD,d’EpifanioA,diBartolomeo E,BalestrinoG,LicocciaSandTraversaE2009Im provingtheperformanceofhightemperatureprot onicconductor(HTPC)electrolytesforsolidoxi defuelcell(SOFC)applicationsKeyEng.Mater **421**–422336–9
- [36] SunW,ShiZ,LiuM,BiLandLiuW2014Aneasil ysintered,chemicallystable,bariumzirconate- basedprotonconductorforhigh- performanceproto- conductingsolidoxidefuelcellsAdv.Funct.Mater.**24**5695–702

- [37] FabbriE,DepifanioA,DibartolomeoE,LicocciaS andTraversaE2008Tailoringthechemicalstabilit yof Ba(Ce<sub>0.8-x</sub>Zr<sub>x</sub>)Y<sub>0.2</sub>O<sub>3-δ</sub>protonicconductorsforintermediateattemperaturesolidoxidefuelcells(IT-SOFCs)SolidStateIon.**179**558–64
- [38] BiL,FabbriE,SunZandTraversaE2011Sinteractivity,protonconductivityandchemicalstabilityofBaZr<sub>0.7</sub>In<sub>0.3</sub>O<sub>3-δ</sub>forsolidoxidefuelcells(SOFCs)SolidStateIon.**196**59–64
- [39] VahidMohammadiAandChengZ2015Fundamentalsofsynthesis,sinteringissues, andchemicalstabilityofBaZr<sub>0.1</sub>Ce<sub>0.7</sub>Y<sub>0.1</sub>Yb<sub>0.1</sub>O<sub>3-δ</sub>protonconductingelectrolyteforSOFCsJ.Electrochem.Soc.**162**F803–11
- [40] SawantP,VarmaS,WaniBNandBharadwajSR 2012Synthesis,stabilityandconductivityofBa Ce<sub>0.8-x</sub>Zr<sub>x</sub>Y<sub>0.2</sub>O<sub>3-δ</sub>aselectrolyteforprotonconductingSOFCInt.J.Hydrog.Energy**37**3848–56
- [41] KreuerKD2003Proton-conductingoxidesAnnu.Rev.Mater.Res.**33**33 3–59
- [42] YamazakiY,Hernandez-SanchezRandHaileSM2009Hightotalprotonconductivityinlarge-grainedyttrium-dopedbariumzirconateChem.Mater.**21**2755–62
- [43] LarringYandNorbyT1997Theequilibriumbetweenwatervapour,protons,andoxygenvacanciesinrareearthoxideSolidStateIon.**97**523–8
- [44] BjørheimTS,LøkenAandHaugsrudR2016OntherelationshipbetweenchemicalexpansionanddehydrationthermodynamicsofprotonconductingperovskitesJ.Mater.Chem.A**45**917–24
- [45] KreuerKD1999Aspectsoftheformationandmobilityofprotonicchargecarriersandthestabilityofperovskite-typeoxidesSolidStateIon.**125**285–302
- [46] BjørheimTS,RahmanSM,ErikssonSG,KneeCSandHaugsrudR2015Hydrationthermodynamicsofthe protonconductingoxygen-deficientperovskiteseriesBaTi<sub>1-x</sub>M<sub>x</sub>O<sub>3-x/2</sub>withM=InorScInorg.Chem.**54**2858–65
- [47] LøkenA,BjørheimTSandHaugsrudR2015ThepivotalroleofthedopantchoiceontherandomicsofhydrationandassociationsinprotonconductingBaCe<sub>0.9</sub>X<sub>0.1</sub>O<sub>3-δ</sub>(X=Sc,Ga,Y,In,GdandEr)J.Mater.Chem.A**32**3289–98
- [48] EiseleS,DraberFMandGrieshammerS2021Theeffectofionicdefectinteractionsonthehydrationofyttrium-dopedbariumzirconatePhys.Chem.Chem.Phys.**23**4882–91
- [49] PutilovLPandTsidilkovskiVI2019Impactofboundionicdefectsonthehydrationofacceptordopedproton-conductingperovskitesPhys.Chem.Chem.Phys.**21**6391–406
- [50] YamazakiY,BabiloPandHaileSM2008Defectchemistryoffyttrium-dopedbariumzirconate:athermodynamicanalysisofwateruptakeChem.Mater.**20**6352–7
- [51] HyodoJ,KitabayashiK,HoshinoK,OkuyamaY andYamazakiY2020Fastandstableprotonconductioninheavilyscandium-dopedpolycrystallinebariumzirconateatintermediateattemperaturesAdv.EnergyMater.**10**200213
- [52] GianniciF,LongoA,BalernaA,KreuerK-DandMartoranaA2009ProtodynamicsinIn:BaZrO<sub>3</sub>:insights on the atomic and electronic structure from x-rayabsorptionspectroscopyChem.Mater.**21**26 41–9
- [53] OikawaIandTakamuraH2015Correlationamongoxygenvacancies,protonicdefects, andtheacceptordopantinSc-dopedBaZrO<sub>3</sub>studiedby<sup>45</sup>ScnuclearmagneticresonanceChem.Mater.**27**6660–7